Radiative electron-capture processes in zero- and one-electron heavy-ion collisions with He

H. Tawara,* Patrick Richard, and K. Kawatsura†
Department of Physics, Kansas State University, Manhattan, Kansas 66506
(Received 21 October 1981)

The x rays from radiative electron capture (REC) have been observed under single-collision conditions for F^{8+} and F^{9+} ions incident on a He-gas target in the collision energy range 15 to 40 MeV. The peak energies of the REC x rays have been found to change linearly with the projectile ion energies. From extrapolation to the zero projectile energy, the binding energies of the 1s-shell electrons have been estimated to be 0.97 ± 0.02 keV for F^{7+} and 1.08 ± 0.02 keV for F^{8+} ions. These values are in agreement with theoretical predictions. It is found that the width of the REC x-ray peak for F^{9+} ions is broader than that for F^{8+} ions in contrast with a model for REC. The production cross sections of the REC x rays for F^{9+} ions are in reasonable agreement with the Bethe-Salpeter calculation. The total REC x-ray-production cross sections for F^{8+} and F^{9+} are compared with the total electron-capture cross sections.

I. INTRODUCTION

In energetic heavy-ion—atom collisions, observations of various types of x rays, in addition to the well-known atomic deexcitation x rays originating from projectile ions or from target atoms[1,2] have been reported: (i) molecular orbital x rays produced in transitions between molecular states of quasimolecules formed during ion-atom collisions,[3] (ii) x rays due to radiative electron capture (REC) originating from the capture of a target electron into some state of a highly ionized projectile ion,[4] and (iii) bremsstrahlung due to electrons knocked out of the target atom.[5] The distributions of these x-ray energies are much broader than that of the characteristic x rays and are continuous over a wide range of energy. Molecular orbital x rays reported in 1972 have been intensively investigated and are particularly interesting in very heavy-ion—atom collisions.[2] Broad bands of x rays due to the radiative electron capture in heavy-ion collisions have been observed in 1972. Since then, some investigations of this process have been reported.[6–10] In all but one[8] of these works, either solid targets or gas cell windows for passage of the projectile ions were used. Therefore, it was impossible to know the charge state of the projectile ions giving rise to the REC x rays. Therefore, the observed data could only provide information averaged over the charge states of the ions.

In the present work, we report measurements and analyses of the x rays produced in the radiative electron-capture process under single-collision conditions in F^{9+} and F^{8+} ions incident on a He-gas target.

II. THEORETICAL BACKGROUND

The radiative capture process (REC) of a free electron into a discrete state of an ion has been theoretically treated first by Bethe and Salpeter[11] as the recombination process. They obtained the REC cross section for bare ions plus a free electron [see Eq. (2) below]. In the present case, the electrons to be captured are not free but bound to a nucleus, and therefore have a momentum distribution. Here we follow the discussions given by Kleber and Jakubassa.[12]

If the velocity of the ion v_0 is greater than the orbital velocity of the target electron which is to be captured, the cross section for the REC process for a bare heavy ion (nuclear charge: Z_1) and a bound electron is given, based upon the impulse approximation, as follows:

$$\frac{d^2\sigma}{d\Omega\, d\hbar\omega} = \int d^3\vec{p}\,\frac{d\sigma(\mathrm{REC})}{d\Omega}\,|\psi_i(\vec{p}-\vec{p}_0)|^2\delta(E_f-E_i)\,, \tag{1}$$

$$\frac{d\sigma(\mathrm{REC})}{d\Omega} = 1.09F(\eta)\sin^2\theta/(1-\beta\cos\theta)^4 \times 10^{-21}\ \mathrm{cm}^2 , \quad (2)$$

$$F(\eta)=\left[\frac{\eta^3}{1+\eta^2}\right]^2 \frac{\exp[-4\eta\arctan(1/\eta)]}{1-\exp(-2\pi\eta)} , \quad (3)$$

$$\eta=Z_1e^2/\hbar v_0, \quad \beta=v_0/c ,$$

where $d\sigma(\mathrm{REC})/d\Omega$ is the recombination cross section for the bare ion and a free electron as calculated by Bethe and Salpeter, $|\psi_i(\vec{p})|^2$ is the initial electronic momentum distribution of the electron before capture which peaks around a momentum $p_0=mv_0$ (m: electron mass) because the electron is moving with this average momentum towards the projectile, E_i and E_f are the total energies of the electron in the initial and final states, respectively, and θ is the angle of the photon emission with respect to the direction of motion of the projectile. Then, the cross section for radiative electron capture into the K shell of a heavy ion is given, using parameters relevant to the collision system, as

$$\frac{d^2\sigma}{d\Omega\, d\hbar\omega} = \left[\frac{d\sigma(\mathrm{REC})}{d\Omega}\right]_{p=p_0+p_{iz}} \times \int d^3p_i\, |\psi_i(p_i)|^2 \times \delta\left[\hbar\omega-\epsilon_f+\epsilon_i-\frac{p_0^2}{2m}-v_0p_{iz}\right] \quad (4)$$

since $d\sigma(\mathrm{REC})/d\Omega$ varies slowly. Here $\hbar\omega$ is the energy of the photon emitted in the REC process, ϵ_i and ϵ_f are the binding energies of electrons in the initial and final states, respectively, and p_{iz} is the momentum component of the electron in the initial state, parallel to the direction of motion of the projectile ion.

Using the Compton profile, $I_i(p_{iz})$, which is the probability function of finding the electron with momentum p_{iz}, the REC cross section at the photon energy $\hbar\omega$ is given as

$$\frac{d^2\sigma}{d\Omega\, d\hbar\omega}=\frac{1}{v_0}\left[\frac{d\sigma(\mathrm{REC})}{d\Omega}\right]_{p=p_0+p_{iz}} I_i(p_{iz}) , \quad (5)$$

where the photon energy is given by

$$\hbar\omega=\epsilon_f-\epsilon_i+(p_0^2/2m)+v_0p_{iz} . \quad (6)$$

The cross section integrated over the photon energy is approximately equal to Eq. (2). As seen in Eq. (5), the energy distribution of the emitted photon in the REC is determined by the capture electron's Compton profile $I_i(p_{iz})$.

It is also seen from Eq. (6) that the photon energy changes linearly with the projectile ion energy [$p_0^2/2m=(m/M)E_0$, E_0: laboratory energy of the incident ion, M: mass of incident ion]. Further, the Compton profile for a hydrogenlike atom is given as

$$I_i(p_{iz})=\frac{8\kappa_i^5}{3\pi(p_{iz}^2+\kappa_i^2)^3} , \quad (7)$$

where $\kappa_i=Z_2^{\mathrm{eff}}me^2/\hbar n$ (Z_2^{eff}: the effective nuclear charge of the target, n: the principal quantum number of the initial state of the electron).

III. EXPERIMENTAL PROCEDURE

The present experiment was performed using fluorine ion beams which were accelerated with the Kansas State University EN tandem Van de Graaff accelerator. F^{8+} and F^{9+} ion beams were obtained after passing the primary beam through a post stripping carbon foil of about 10 μg/cm^2. The beam was then magnetically analyzed and focused by a magnetic quadrupole lens into the target region. Beam intensities varied from about 10 nA at 15 MeV to some hundreds of nA at higher energies.

The ion beams were collimated by two sets of 2.5×2.5 mm^2 square slits, 15 cm apart from each other, before arriving at a single nozzle gas jet target of He which was localized 10 cm behind the last slit. The distance from the switching magnet to the gas nozzle was approximately 15 m and the base pressure in this region of the beam line varied from 2×10^{-7} Torr to 6×10^{-7} Torr depending on the nozzle pressure. The gas jet target was used to obtain a high gas target density in a narrow collision region. The relative pressure of the target He gas was monitored with a thermocouple gauge. The thermocouple gauge located at the roughing end of the diffusion pump directly below the jet nozzle registered in the range from 0 to 80 mTorr. No attempts were made to estimate or determine the pressure in the nozzle region. A test for single-collision conditions was performed by observing the K x-ray and K REC intensities as a function of pressure as shown in Fig. 1 for the case of 30 MeV $F^{9+}+He$. The yield was observed to be linear over the entire range of pressures used in the experiment. Data were obtained at several pressures for most projectile energies and charge states.

X rays produced in the collision were observed

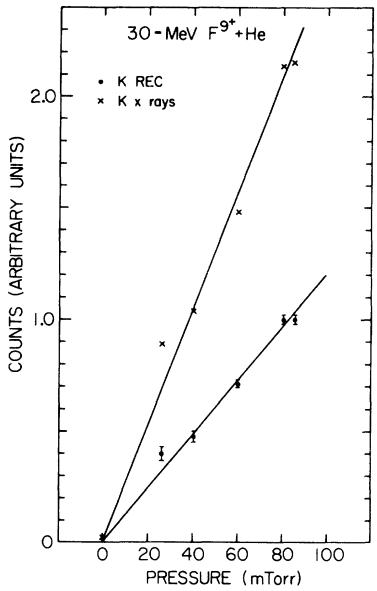

FIG. 1. Observed pressure dependence of the F K x-ray yields and the F K REC x-ray yields in the range of 20 to 80 mTorr are depicted. The solid lines are linear fits to the data.

with an ORTEC Si(Li) x-ray detector which had 200-Å Au electrical contact layer and 1000-Å Si dead layer in addition to a 12.5-μm Be window. An energy calibration and linearity check of the Si(Li) detector plus amplifier system were made using standard Mn $K\alpha$ and $K\beta$ x rays from an ^{55}Fe source and the characteristic x rays from Ca, Ar, Cl, Si, Al, and Mg photoionized by Mn x rays. Typical energy resolution of the Si(Li) detector system was about 180 eV for Mn $K\alpha$ x rays. To reduce background x rays, the ion beams were stopped in a Faraday cup about 1 m behind the collision region. Furthermore, to reduce background x rays originating from the walls of the collision chamber, the Si(Li) detector was collimated with a lucite cap with a hole of 6.25 mm in diameter which limited the view of the Si(Li) detector to a small area of the opposite wall. The effective solid angle extended by the Si(Li) detector was from the geometry estimated to be about 10^{-2} sr.

IV. EXPERIMENTAL RESULTS AND DISCUSSIONS

A. X-ray spectra and normalization procedures

Typical x-ray spectra observed with the Si(Li) detector are shown in Fig. 2 for 15- and 30-MeV F^{8+} and F^{9+} ions incident on a He-gas target. There are two prominent peaks: one at lower energy which is the F K x-ray peak and one at higher energy which is the REC x-ray peak. It is found that the spectrum shape of F K x rays from F^{9+} ion impact does not change significantly with projectile energy because F K x rays in this case are produced only through the electron capture into excited states (nl) over the whole impact energy.[13] The strong peak of F K x rays from F^{9+} ion impact at around channel 128 (1019 eV) is due to a superposition of the $3p$, $4p$, $5p$, ... $\rightarrow 1s$ H-like x-ray transitions and the low-energy shoulder at around channel 103 (825 eV) is due to the $2p \rightarrow 1s$ H-like x-ray transition. On the other hand, the F K x-ray spectra from F^{8+} ion impact are more complicated and change rather significantly with the projectile energy. The peak at around channel 110 (879 eV) at 15-MeV ion impact [see Fig. 2(a)] is mainly due to a superposition of the $1s3p$, $1s4p$, $1s5p$, ... $\rightarrow 1s^2$ He-like x-ray transitions which are produced through electron capture at this bombarding energy. The weak shoulder at around channel 91 (732 eV) is due to the $1s2p \rightarrow 1s^2$ He-like x-ray transition which is also produced through electron capture. At the higher bombarding energy [see Fig. 2(b)], higher-energy transitions due to electron excitation of the F^{8+} ion became more important[14] and gave rise to $2p$, $3p$, $4p$, $5p$, ... $\rightarrow 1s$ H-like x-ray transitions and thus the high-energy shoulder in the x-ray spectrum. Because of this behavior, the position of the strong F K x-ray peak moves toward channel 105 (841 eV), which is close to the position of the $2p \rightarrow 1s$ H-like x-ray transition, as the F^{8+} ion energy is increased. The F^{8+} spectra thus get broader with increasing projectile energy due to the presence of H-like and He-like x-ray transitions with nearly equal probability.

As mentioned above, the observed F K x-ray spectrum is not a single component but consists of a number of peaks originating from different transitions.[13] For example, F K x-ray spectra from F^{9+} ion impact could be decomposed into five transition peaks, namely, $2p$, $3p$, $4p$, $5p$, and the average of $6p$ to series limit $\rightarrow 1S$ transitions which all originate in the electron-capture process. In order to get a better fit, it was necessary to add a peak due to the $1s2p \rightarrow 1s^2$ transition which is formed through one-electron capture to F^{8+} ions produced in a previous electron capture to the incident F^{9+} ions. The analyzed results show that contribution from the $1s2p \rightarrow 1s^2$ transition amounts to about 2% in the observed total x-ray spectrum intensity. The actual

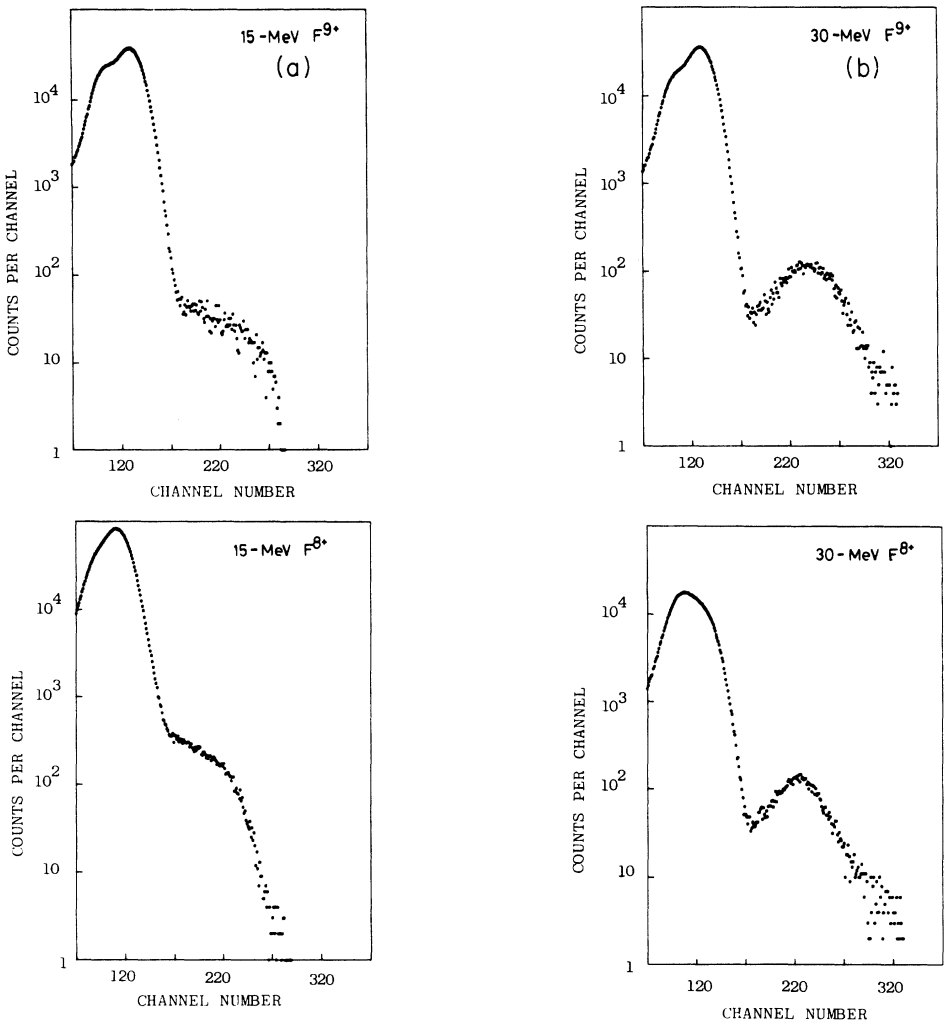

FIG. 2. Typical x-ray spectra from F^{8+} and F^{9+} ions incident on a He-gas target at 15 and 30 MeV under single-collision conditions observed with a Si(Li) detector with 12.5-μm Be window. The peak at the left is due to F K x rays and the one at the right is due to the REC x rays.

intensities of these decomposed peaks were obtained after correcting for transmission through the Be window and other dead layers in the Si(Li) x-ray detector which were provided by the manufacturer, using the absorption coefficients for x rays listed by Henki and Elgin and by Storm and Israel.[15] These corrected intensities for the different transitions compare favorably with those previously measured using a high-resolution x-ray crystal spectrometer.[13]

The relative cross sections for production of F K x rays in $F^{9+}+He$ collisions as a function of the projectile ion energy are in good agreement with previous measurements.[16] To set absolute values of the cross sections, the measured F K x-ray yield in the $F^{9+}+He$ collision was normalized to the cross section at 15 MeV obtained by Guffey *et al.*[16] By taking into account uncertainties in the thickness of the Be window and others, uncertainties in the absolute values of the cross sections in F K x-ray and REC x-ray productions are estimated to be about 50%.

B. REC x-ray peak energy

As discussed above [Eq. (6)], the peak energy of the REC x rays changes with projectile energy and is given from the relevant parameters as

$$\hbar\omega(\mathrm{REC})=\epsilon_f-\epsilon_i+(m/M)E_0\ . \tag{8}$$

ϵ_f corresponds to the binding energy of the electron in the 1s shell of the projectile ion and ϵ_i that of the electron in the 1s shell of the He atom (24.5 eV). The observed results of the REC x-ray peak energy in F^{8+} and F^{9+} ion impact on He gas are shown in Fig. 3 as a function of the projectile energy.[17] As expected in Eq. (8), the peak energy of the REC x rays decreases linearly with decreasing projectile energy for both F^{8+} and F^{9+} ions. Finally the curves intercept the ordinate at the zero projectile energy. This interception at $E_0=0$ gives the difference between the binding energies of the electron in the initial and final states. From the intercepts for F^{8+} and F^{9+} ion impact, the binding energies of the 1s-shell electron are found to be $\epsilon_f=0.97\pm0.02$ keV for a F^{7+} ion and 1.08 ± 0.02 keV for a F^{8+} ion. These values are in reasonable agreement with theoretical values of 0.952 and 1.103 keV, respectively.[18] The He-like binding in F^{7+} has been reported by Tyren[19] as 0.9536 keV and by Kauffman *et al.*[20] as 0.9545 keV from measurements of the two-electron x-ray series limit. The H-like binding in F^{8+} has also been reported by Kauffman *et al.*[20] as 1.103 keV from measurement of the one-electron x-ray series limit. The independent determination of the binding energies for H- and He-like ions from REC measurements is possible only when a gas target is used for measurement of the REC x rays using the charge-selected projectile ions and the single-collision condition is satisfied.

C. REC x-ray width

The broadening of the REC x-ray peaks comes from the fact that the electron to be captured has some momentum distribution in the initial state. From the most simplified consideration, the full width at half maximum (FWHM) of the REC x rays is given as [see Eq. (6)]

$$\Delta\hbar\omega(\mathrm{FWHM})=2v_0p_{iz}=2[4(m/M)E_0\epsilon_i]^{1/2}\ . \tag{9}$$

A factor of 2 comes from two directions of the initial momentum p_{iz} of the electron. In Fig. 4 are shown the results of measurements of FWHM of the REC x rays in F^{9+} and F^{8+} ion impact on a He-gas target as a function of projectile energy.[17] The predicted FWHM based on Eq. (9) is also shown in Fig. 4 and is systematically about 15% larger than the measured values for F^{9+} ions. Theoretical values of FWHM, under the assumption that the initial momentum distribution of the electron has the Compton profile of H-like ions ($Z_2^{\mathrm{eff}}=Z_2$), are also shown in Fig. 4. These are smaller than the experimental values for F^{9+} ions by $\sim10\%$. According to the theory discussed above [Eq. (9)], the REC width should be independent of the binding energy of electrons in the projectile ions and therefore, no difference is expected in the FWHM of the REC peaks for F^{9+} and F^{8+} ions. However, the measured data indicate that the FWHM of REC peaks for F^{8+} ions is systematically 25% smaller than that for F^{9+} ions. This difference may be due to the difference of the effective

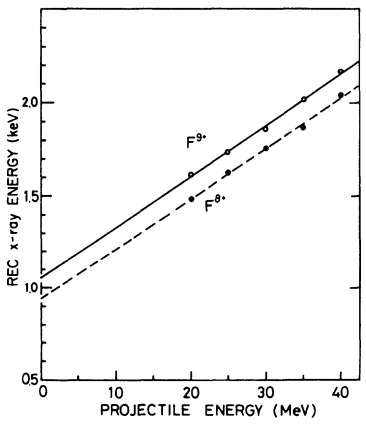

FIG. 3. Peak energy of the REC x rays from F^{8+} and F^{9+} ions incident on a He-gas target as a function of the projectile energy.

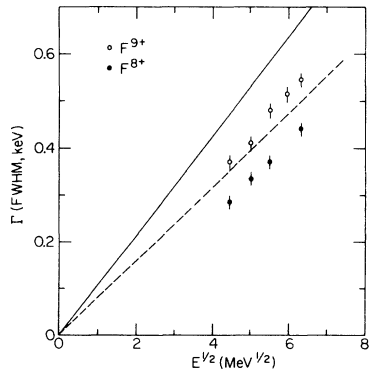

FIG. 4. FWHM of the REC x rays from F^{8+} and F^{9+} ions incident on a He-gas target as a function of the projectile energy. Solid line: prediction based on Eq. (9). Dashed line: prediction assuming the Compton profile with $Z_2^{\mathrm{eff}}=Z_2$.

nuclear charge of the projectiles. In fact, the ratio of the effective charges is very close to the ratio of the experimental values of the FWHM. It is also noted that the ratios of the FWHM of the REC to the REC peak energy are almost identical for both F^{9+} and F^{8+} ions.

D. REC spectrum

The REC spectrum (energy distribution of REC x rays) reflects the distribution of the electron momentum in the target atom and, as discussed above, the REC spectrum shape is governed by the Compton profile function $I_i(p_{iz})$ [Eq. (5)]. In the present target of He, the REC spectrum should be simple because the electrons are in a single shell, i.e., the K shell. In Fig. 5 is shown the observed REC x-ray spectrum at 30-MeV F^{9+} ion impact on He, together with the calculated (normalized) spectra with the effective target nuclear charge $Z_2^{\text{eff}}=Z_2-0.3$ and Z_2 and also the curve fitted to the experimental data. The experimental REC spectrum is similar to the calculated spectrum with the unscreened nuclear charge $Z_2^{\text{eff}}=Z_2$. The experimental spectrum is broader than the calculated spectrum with the screened nuclear charge $Z_2^{\text{eff}}=Z_2-0.3$. This may indicate that the REC process into the K shell of the projectile from the K shell of the simple target atom at relatively high impact energy (1.6 MeV/amu) effectively occurs at impact parameters smaller than the K-shell radius of the target atom, as noted theoretically by Kleber and Jakubassa,[12] meaning that the screening of the nucleus by the K-shell electrons is less effective. An additional effect could be the distortion of the target atomic level by the highly charged projectile prior to electron transfer. Therefore, a different effective charge for F^{9+} and F^{8+} can result in a different atomic distortion (thus different binding energy). This, in turn, may give a narrower REC peak for F^{8+} than for F^{9+} ions. It would be interesting to investigate the impact-parameter dependence of the REC process in heavy-ion collisions for different projectiles.

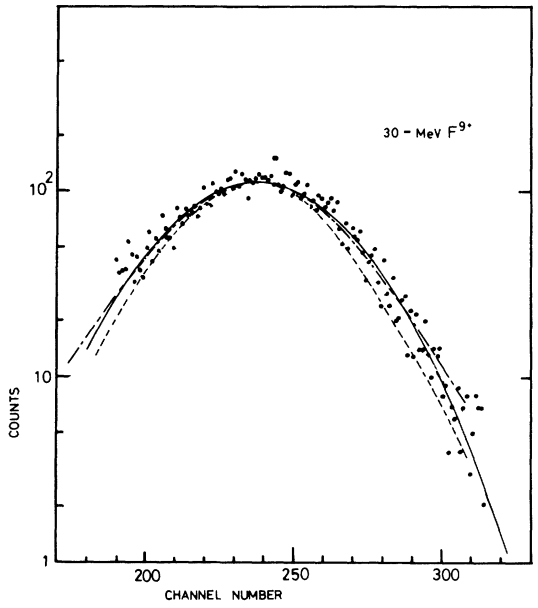

FIG. 5. Spectra of the REC x rays at 30-MeV F^{9+} ions on He-gas target. ●: experimental points. Solid line: fitted curve to data. Dot-dashed line: prediction assuming the Compton profile with $Z_2^{\text{eff}}=Z_2$. Dashed line: prediction assuming the Compton profile with $Z_2^{\text{eff}}=Z_2-0.3$.

E. REC cross section

Because there are two $1s$-shell vacancies in F^{9+} ions, compared with one vacancy in F^{8+} ions, it is expected that the REC x-ray production cross sections for F^{9+} ions are equal to twice those for F^{8+} ions. The measured REC x-ray production cross sections for F^{9+} and F^{8+} ions at 90° are shown in Fig. 6. The measured REC cross sections for F^{9+} ions are slightly larger than twice those for F^{8+} ions, though data are rather scattered. In Fig. 6 is also shown the Bethe-Salpeter prediction which is based upon the free-electron model. The agreement

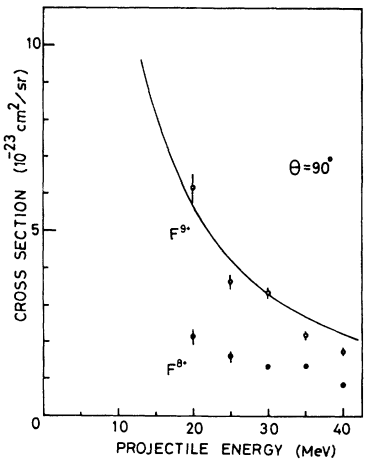

FIG. 6. Cross section of the REC x rays from F^{8+} and F^{9+} ions on He at 90°. Solid line: prediction of the Bethe-Salpeter calculation.

between data and the Bethe-Salpeter calculation for F^{9+} ions is reasonably good. An additional overall uncertainty of about 50% in the absolute values of the measured cross sections in the present experiment must be taken into account in the comparison. The indicated errors are due to statistical and fitting errors only. The energy dependence of the REC x-ray cross sections is well reproduced with the Bethe-Salpeter prediction.

F. Comparison of REC cross sections with total electron capture

The process of electron capture into the $1s$ state of a bare ion impinging on a simple target atom like H or He can proceed either by nonradiative electron capture or by radiative electron capture. Then, the total electron-capture cross section into the $1s$ state can be written as

$$\sigma_Z(1s)=\sigma_Z^K(\mathrm{NR})+\sigma_Z^K(\mathrm{REC}) , \tag{10}$$

where $\sigma_Z^K(\mathrm{NR})$ and $\sigma_Z^K(\mathrm{REC})$ are the cross sections for the nonradiative and radiative electron-capture processes for the bare ion, respectively. The cross section $\sigma_Z^K(\mathrm{REC})$ can be measured for heavy ions, as mentioned already. However, the cross sections $\sigma_Z(1s)$ and $\sigma_Z^K(\mathrm{NR})$ cannot be determined directly. On the other hand, the total one-electron-capture cross section $\sigma_{Z,Z-1}$ ions can be measured.[21]

Similar arguments can be made for the electron capture by one-electron heavy ions as follows:

$$\sigma_{Z-1}(1s)=\sigma_{Z-1}^K(\mathrm{NR})+\sigma_{Z-1}^K(\mathrm{REC}) . \tag{11}$$

For the present collision systems, the existing measured quantities[21] are shown in Fig. 7. It is found that the REC cross sections $\sigma_Z(\mathrm{REC})$ and $\sigma_{Z-1}(\mathrm{REC})$ measured in the present work are more than three orders of magnitude smaller than the total capture cross sections $\sigma_{Z,Z-1}$ and $\sigma_{Z-1,Z-2}$, respectively. As shown in Fig. 6, the ratios of REC cross sections for F^{9+} compared to F^{8+} are slightly larger than two. However, the ratios of total electron-capture cross sections $\sigma_{9,8}/\sigma_{8,7}$ are, on the average, 1.4 ± 0.1 for He in the present energy range, indicating that the total electron-capture cross sections scale as Z_1^3, as previously discussed,[22] and the screening by one $1s$-shell electron is insignificant ($Z_1^{\mathrm{eff}}=8$ for F^{8+} ions).

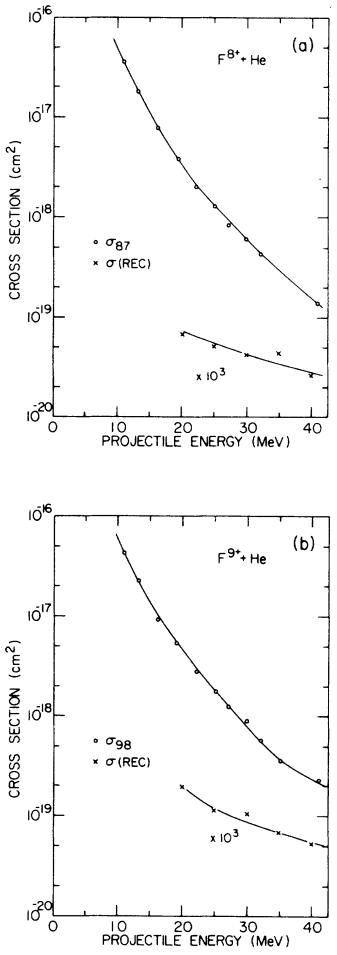

FIG. 7. Comparison of cross sections for various processes involving F^{8+} and F^{9+} ions in collision with He-gas target. ○: total electron-capture cross section. ×: total REC x-ray production cross section.

V. CONCLUSION

In the present work we have measured the x rays from the REC process, for the first time, under single-collision conditions in F^{8+}, F^{9+}+He collisions in the energy range 15–40 MeV. The REC x-ray peak energies have been found to change linearly with the energy of projectile ions. From the intercepts at the zero projectile energy, the binding energies of the $1s$-shell electron have been determined to be 0.97 ± 0.02 and 1.08 ± 0.02 keV for F^{7+} and F^{8+} ions, which are in reasonable agreement with theoretical estimates. The FWHM of the REC x-ray peaks is larger for F^{9+} ions than for F^{8+} ions. The REC x-ray production cross sections at 90° for F^{9+} ions are favorably compared with the Bethe-Salpeter calculation. The total REC cross sections for F^{8+} and F^{9+} ions have been found to be more than three orders of magnitude smaller than the total electron-capture cross sections even at the highest projectile energy. It is concluded from the

present work that measurements of the peak energy of the REC photons from highly ionized heavy ions in collision with gas target as a function of the ion energy could be a useful method for determining the binding energy of few-electron ions. It is worthwhile to point out that the calculations by Briggs and Dettmann[23] and by Shakeshaft and Spruch[24] show that the cross sections for the REC process become dominant over those for the nonradiative process at higher collision energies. It would therefore be interesting to measure the x rays from the REC process at energies much higher than in the present study.

We propose that the observed difference in the widths of the REC peaks for F^{9+} and F^{8+} ions is due to the difference in the effective charge of the projectile ions which in turn produces different atomic distortions of the He electrons prior to electron transfer. The near agreement between the experiment F^{9+} REC peak width and the prediction using the Compton profile may indicate that the capture occurs at impact parameters near the He K-shell radius. Finally, it is proposed that the impact-parameter dependence of the REC x-ray yields be investigated in order to understand the REC process more thoroughly.

ACKNOWLEDGMENT

This work was supported by the U.S. Department of Energy, Division of Chemical Sciences.

---

*Present address: Kyushu University, Fukuoka 812, Japan.

†Present address: Japan Atomic Energy Research Institute, Tokai Ibaraki 319-11, Japan.

[1]P. Richard, *Atomic Inner Shell Processes,* edited by B. Crasemann (Academic, New York, 1975), p. 73.

[2]P. H. Mokler and F. Folkman, *Structure and Collisions of Ions and Atoms,* edited by I. A. Sellin (Springer, Berlin, 1978), p. 201.

[3]F. W. Saris, W. F. van der Weg, H. Tawara, and R. Laubert, Phys. Rev. Lett. 28, 717 (1972); J. S. Greenberg, *Electronic and Atomic Collisions,* edited by N. Oda and K. Takayanagi (North-Holland, Amsterdam, 1980), p. 351; J. Reinhardt, W. Greiner, B. Müller, and S. Soff, *ibid.*, p. 369.

[4]H. W. Schnopper, H. D. Betz, J. P. Delvaille, K. Kalata, A. R. Sohval, K. W. Jones, and H. E. Wegner, Phys. Rev. Lett. 29, 898 (1972).

[5]F. Folkmann, C. Gaarde, T. Huus, and K. Kemp, Nucl. Instrum. Methods 116, 487 (1974); K. Ishii, S. Morita, and H. Tawara, Phys. Rev. A 13, 131 (1976).

[6]P. Kienle, M. Kleber, B. Povh, R. M. Diamond, F. S. Stephens, E. Grosse, M. R. Maier, and D. Proetel, Phys. Rev. Lett. 31, 1099 (1973).

[7]H. W. Schnopper and J. P. Delvaille, *Atomic Collisions in Solids,* edited by S. Datz *et al.* (Plenum, New York, 1975), p. 481.

[8]A. R. Sohval, J. P. Delvaille, K. Kalata, K. Kirby-Docken, and H. W. Schnopper, J. Phys. B 9, L25 (1976).

[9]J. Lindskog, J. Phil, R. Sjödin, A. Marelius, K. Sharma, and R. Hallin, Phys. Scr. 14, 100 (1976); J. A. Tanis and S. M. Shafroth, Phys. Rev. Lett. 40, 1174 (1978).

[10]R. Schule, H. Schmidt-Böcking, and I. Tserruya, J. Phys. B 10, 889 (1977).

[11]H. E. Bethe and E. E. Salpeter, Handb. Phys. 35, 408 (1957).

[12]M. Kleber and D. H. Jakubassa, Nucl. Phys. A 252, 152 (1975).

[13]H. Tawara, P. Richard, K. A. Jamison, T. J. Gray, J. Newcomb, and C. Schmiedekamp, Phys. Rev. A 19, 1960 (1979).

[14]H. Tawara, P. Richard, K. A. Jamison, and T. J. Gray, J. Phys. B 11, L615 (1978).

[15]B. L. Henke and R. L. Elgin, Adv. X-Ray Anal. 13, 639 (1972); E. Storm and H. I. Israel, Nucl. Data Sect. A 7, 565 (1970).

[16]J. A. Guffey, L. D. Ellsworth, and J. R. Macdonald, Phys. Rev. A 15, 1863 (1977); J. A. Guffey, thesis, Kansas State University, 1976 (unpublished).

[17]K. Kawatsura, H. Tawara, and Patrick Richard, IEEE Trans. Nucl. Sci. NS-28, 1053 (1981).

[18]C. P. Bhalla (private communication); and G. W. Erickson, J. Phys. Chem. Ref. Data 6, 831 (1977).

[19]F. Tyren, Nova Acta Regiae Soc. Sci. Ups. 12, 25 (1940).

[20]R. L. Kauffman, C. W. Woods, F. F. Hopkins, D. O. Elliott, K. A. Jamison, and P. Richard, J. Phys. B 6, 2197 (1973).

[21]R. Dillingham, H. Tawara, and Patrick Richard, Phys. Rev. A 24, 1237 (1981).

[22]H. Tawara, Phys. Lett. 71A, 208 (1979).

[23]J. S. Briggs and K. Dettmann, Phys. Rev. Lett. 33, 1123 (1974).

[24]R. Shakeshaft and L. Spruch, Rev. Mod. Phys. 51, 369 (1979).